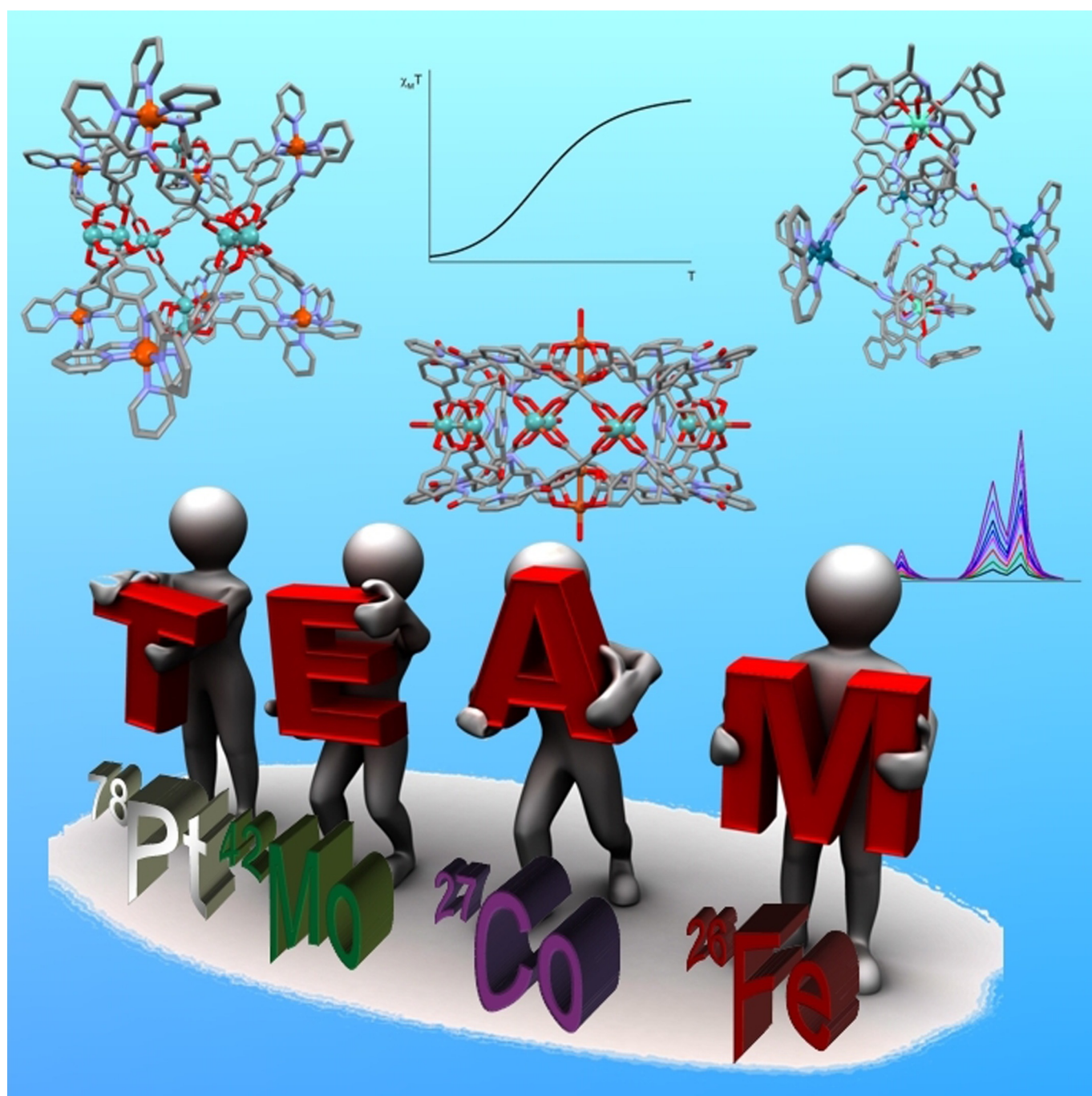


■ Supramolecular Chemistry | *Reviews Showcase* |🏆 **Better Together: Functional Heterobimetallic Macrocyclic and Cage-like Assemblies**Matthias Hardy and Arne Lützen*^[a]

Abstract: Metallosupramolecular chemistry has attracted the interest of generations of researchers due to the versatile properties and functionalities of oligonuclear coordination complexes. Quite a number of different discrete cages were investigated, mostly consisting of only one type of ligand and one type of metal cation. Looking for ever more complex structures, heterobimetallic complexes became more and more attractive, as they give access to new structural motifs and functions. In the last years substantial success

has been made in the design and synthesis of cages consisting of more than one type of metal cations, and a rapidly growing number of functional materials has appeared in the literature. This Minireview describes recent developments in the field of discrete heterometallic macrocycles and cages focusing on functional materials that have been used as host-systems or as magnetic, photo-active, redox-active, and even catalytically active materials.

Introduction

In the past decades, coordination-driven self-assembly of organic ligands and metal cations to well-defined and often aesthetically very appealing discrete 2D- and 3D-architectures has been a widely studied and still is a highly active field in supramolecular chemistry. Besides their pure aesthetics, however, a careful design and choice of the ligand structures and the metal centers also offer unique chances to introduce certain functions that are hardly accessible employing covalent approaches.

Many advances were made in making self-assembly processes predictable and design approaches like the symmetry-interaction approach,^[1] the molecular-library approach^[2] and the molecular paneling approach^[3] soon became generally used tools in planning sophisticated supramolecular structures. Many reviews were published on metallosupramolecular cages and macrocycles with different functionalities, like host–guest systems, photo- or redox-active complexes, magnetic molecules or even molecular flasks.^[4–8]

However, most of the work in this field was done with homometallic structures. As increasing complexity is one major goal that drives supramolecular research, there is a growing interest in systems that consist of more than one type of metal cation over that past two decades. Significant progress in planning heterobimetallic structures allows for the reliable synthesis of such structures. Particularly, the complex-as-a-ligand strategy and the use of hard and soft metal cations or the use of metal cations that prefer different coordination geometries are common approaches to successfully distinguish between

two different metal cations. There are already some excellent reviews in literature^[5,9–11] that discuss the structural aspects and synthetic strategies in detail with beautiful examples, and therefore, these aspects will not be discussed in detail herein.

Clearly, the combination of two different metal cations in a single discrete aggregate largely increases the accessibility of new structural motifs and geometries. To date, manifold structures were described, amongst others macrocycles,^[12–16] helicates,^[17–19] tetrahedra,^[20] trigonal bipyramids,^[12,21–23] cubic^[21,22,24] and prismatic cages,^[25] and unique assemblies like adamantoid^[26] cages and waterwheel-, tweezer- and butterfly-shaped complexes.^[27]

Using two different metal cations that prefer different coordination spheres, however, also allows for new strategies to achieve high-fidelity self-sorting in complicated situations like five-component,^[28] or even six-component systems,^[29] as nicely demonstrated by Schmittel and co-workers.

Moreover, heterobimetallic systems proved very useful in the synthesis of advanced mechanically interlocked structures, like grid catenanes^[30] and even the templated construction of borromean rings^[31,32] and Solomon links.^[33]

In the following, however, we will concentrate on the discussion of the growing field of functional aspects of heterobimetallic assemblies rather than just on their astonishing discrete 2D- and 3D-structures. In case a metallosupramolecular cage is 'just' used as a container molecule, the nature of the used metal cations might be negligible, but when it comes to certain functionalities, the nature of the metal cations is of major importance and apparently, the use of two different metal cations can lead to strongly improved properties or even the emergence of new ones. Thereby, we will focus on cage-(to-cage) transformations, host–guest interactions, magnetic and photophysical properties, redox activity and catalytic activity.


By discussing recent examples for different sorts of properties, we wish to give insight into the broad and manifold area of functional heterobimetallic assemblies.


Functional Heterobimetallic Assemblies


Cage transformations

Complex-to-complex transformations can be seen as a molecular reaction, where building blocks are exchanged in order to transform one reversibly assembled complex into another

[a] M. Hardy, Prof. Dr. A. Lützen
Kekulé-Institut für Organische Chemie und Biochemie
Universität Bonn
Gerhard-Domagk-Str.1, 53111 Bonn (Germany)
E-mail: arne.luetzen@uni-bonn.de

 The ORCID identification number(s) for the author(s) of this article can be found under:
<https://doi.org/10.1002/chem.202001602>.

 © 2020 The Authors. Published by Wiley-VCH GmbH. This is an open access article under the terms of Creative Commons Attribution NonCommercial License, which permits use, distribution and reproduction in any medium, provided the original work is properly cited and is not used for commercial purposes.

 Selected by the Editorial Office for our Showcase of outstanding Review-type articles (www.chemeurj.org/showcase).

upon exposure to a chemical stimulus. Clearly, one prerequisite is that the overall situation before the transformation is less favored, than the situation afterwards, in order to provide a sufficient driving force for these thermodynamically controlled processes.

This strategy is also a powerful approach to access heterobimetallic complexes as can be seen from the striking example with an unusual cage geometry that was reported from the group of Zhou in 2014.^[34] Here, metal ions could be exchanged. Reaction of protonated **1** with $\text{Mo}_2(\text{OAc})_4$ at 85 °C yielded the core-shell molecular assembly **2**, where two Mo_2 units are bridged by four ligands and this 'core' was surrounded by an additional $(\text{Mo}_2)_4(\text{L})_8$ ring as a shell (Figure 1). Therefore, in the overall assembly, two conformations of the ligand **1** can be found. When crystals of **2** were exposed to a solution of $\text{Cu}(\text{NO}_3)_2$ in DMF for only six hours, partial metathesis was observed. This single crystal to single crystal metathesis gave rise to heterobimetallic $[(\text{Mo}_2\text{L}_2)_4][(\text{Cu}_2\text{L}_2)_2]$ assembly **3** where exclusively the metal units of the core were exchanged. This behavior was attributed to tension in the core assembly with Mo_2 units that is released, if more flexible Cu_2 moieties are incorporated.

Ligand building block exchanges become possible, when the subcomponent self-assembly strategy^[35] is used to construct cages. An example of a sequence of cage-to-cage transformations from a monometallic to a heterobimetallic cage and finally to another monometallic one was introduced by the group of Nitschke.^[36] The homometallic tetrahedron **4** is rather labile due to the long bridging ligands and can incorporate the C_4 symmetric metalloligand **5**, which results in the formation of the heterobimetallic cubic cage **7**, containing eight iron(II) and six platinum(II) cations. This reaction releases twelve equivalents of the long, linear diamine **6**. However, when **7** was then treated with the shorter diamine **8** the metalloligand **5** is again released and **8** was incorporated instead, resulting in the formation of the smaller and more stable homometallic tetrahedral cage **9** (Scheme 1).

Another example of a dynamic heterobimetallic system, consisting of a cube and a trigonal bipyramid, that allows for cage-to-cage transformations could be presented by our group recently.^[37] Ligand fragment exchanges were possible due to a sterically strained coordination sphere around iron(II) cations, caused by crowded ligands with methyl groups. When **11** or **15** were treated with an analogous less bulky non-methylated building block, the systems incorporated the new building block releasing the less favorable subcomponent. The reduction of steric strain might be the driving force in this case and eventually resulted in a change of the spin state of iron(II) cations from high-spin in strained cages to low-spin.

Furthermore, this system also allowed for exchanges of intact ligands. When the chelating bidentate ligand dppp (dppp = 1,3-bis(diphenylphosphino)propane) was added to cubic **10** or **11**, the cages were transformed into the trigonal bipyramidal complexes **14** or **15**, since palladium(II) favors the binding of dppp over 4-pyridyl donors. As a side product the metalloligands **12** and **13** were released in this transformation (Scheme 2). These examples, where metal-bridging compo-

nents within a heterobimetallic system were exchanged, nicely demonstrate how dynamic behavior of heterobimetallic systems can be exploited to manipulate their structures in situ.

Host-guest interactions

Metallosupramolecular architectures with well-defined cavities are often suitable for guest encapsulation. This might be employed to manipulate the conformation, stability and reactivity of guest molecules in certain ways.

Besides a large number of homometallic examples, heterobimetallic assemblies were also successfully employed as host-molecules for several guest molecules. The use of two different metal cations offers a versatile strategy for the construction of large cavities from simple building blocks^[38,39] and also for host molecules that feature two accessible cavities for guest uptake.^[40]

An example for the encapsulation of small organic molecules by a heterobimetallic $[\text{Zr}_6\text{Pd}_3]$ trigonal bipyramid was reported by the group of Mukherjee.^[41] The cage **16** was assembled from two C_3 symmetric trinuclear carboxylate-bridged zirconocene-based metalloligands and three *cis*-blocked palladium(II) building blocks. The water-soluble cage was found to be capable to encapsulate water-insoluble small, electron-rich molecules like naphthalene and 2-naphthaldehyde in its hydrophobic cavity in aqueous media (Figure 2a). Also, the subsequent extraction of guest molecules with chloroform was possible, leaving the empty cage in the aqueous phase.

Jin presented a series of heterobimetallic boxes using Cu^{II} -based pyridyl-functionalized β -diketonate metalloligands with

Matthias Hardy studied chemistry at the University of Bonn and received his M.Sc. in 2016, working with Prof. Arne Lützen. Since then he is working on his Ph.D. project focusing on the synthesis and characterization of heterobimetallic assemblies.



Arne Lützen studied chemistry at the University of Oldenburg and obtained his Ph. D. in the field of carbohydrate chemistry. He was a postdoc in the group of Prof. Dr. Julius Rebek, Jr. at the Scripps Research Institute in La Jolla, USA. He then returned to Oldenburg to start his independent research in the field of supramolecular chemistry. In 2006 he became professor of organic chemistry at the University of Bonn. His research interests include various areas of supramolecular chemistry and organic synthesis.



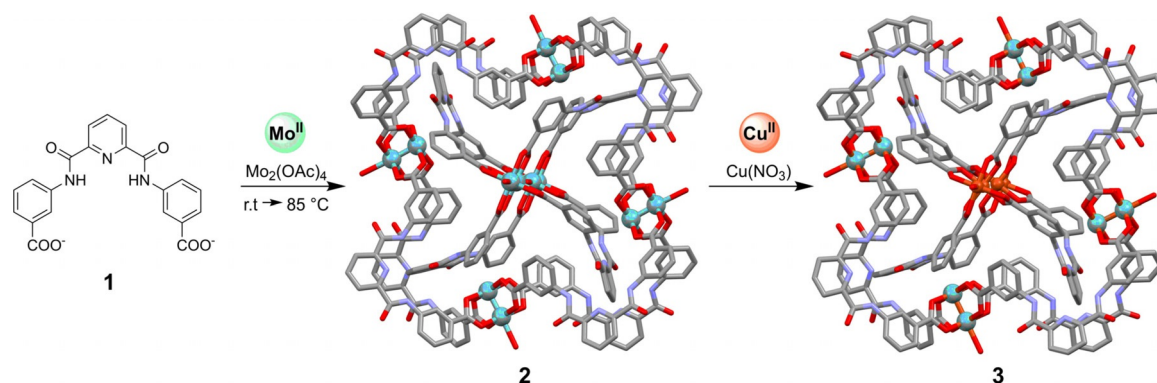
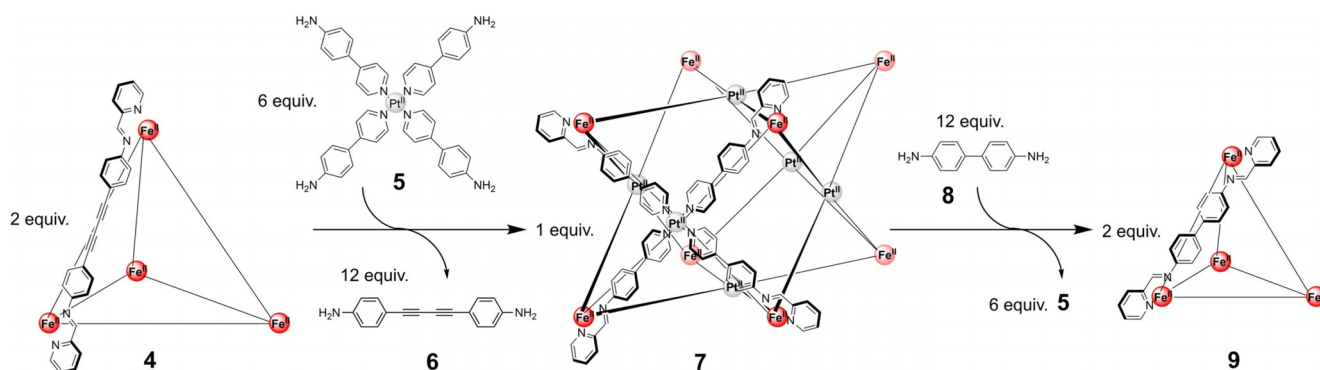
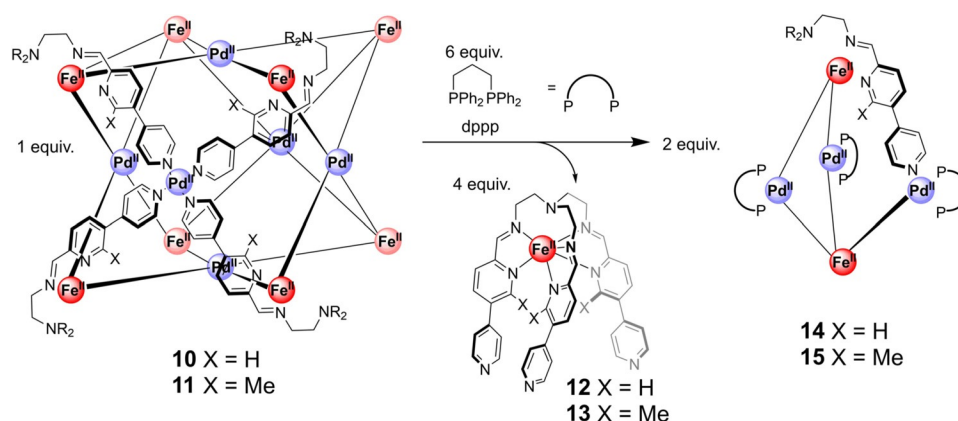


Figure 1. Reaction of **1** with $\text{Mo}_2(\text{OAc})_4$ at high temperatures yielded the core-shell assembly **2** that could be further transformed to heterobimetallic **3** via metathesis of metal ions.^[34]



Scheme 1. Cage-to-cage transformations starting from tetrahedral cage **4** to heterobimetallic **7** upon addition of **5**. Compound **7** could then be transformed to the homometallic tetrahedron **9** upon addition of subcomponent **8**.^[36]



Scheme 2. Transformation of cubic cages **10** and **11** to trigonal bipyramidal assemblies **14** and **15** upon addition of the bidentate ligand dppp .^[37]

half-sandwich Ir, Ru or Rh fragments.^[42–44] They could show that the cage size could be adjusted by choosing different organic ligands so that the size of the inner cavity could be matched to the needs of guest molecules. Using this strategy, they could assemble box-like cage **17** that was able to encapsulate aromatic guests such as pyrene or $[\text{Pt}(\text{acac})_2]$ (Figure 2b).

Severin assembled a heterobimetallic octahedron containing 18 metal centers from a clathrochelate metalloligand with incorporated iron(II) cations^[20,45,46] that was found to be the first metallosupramolecular capsule that successfully encapsulates tetraphenylborate anions.^[47] Cage **18** could bind three BF_4^- anions and one BPh_4^- anion, even from aqueous media (Figure 2c). However, using non-polar solvent mixtures, the observed binding constant for BPh_4^- dropped dramatically, point-

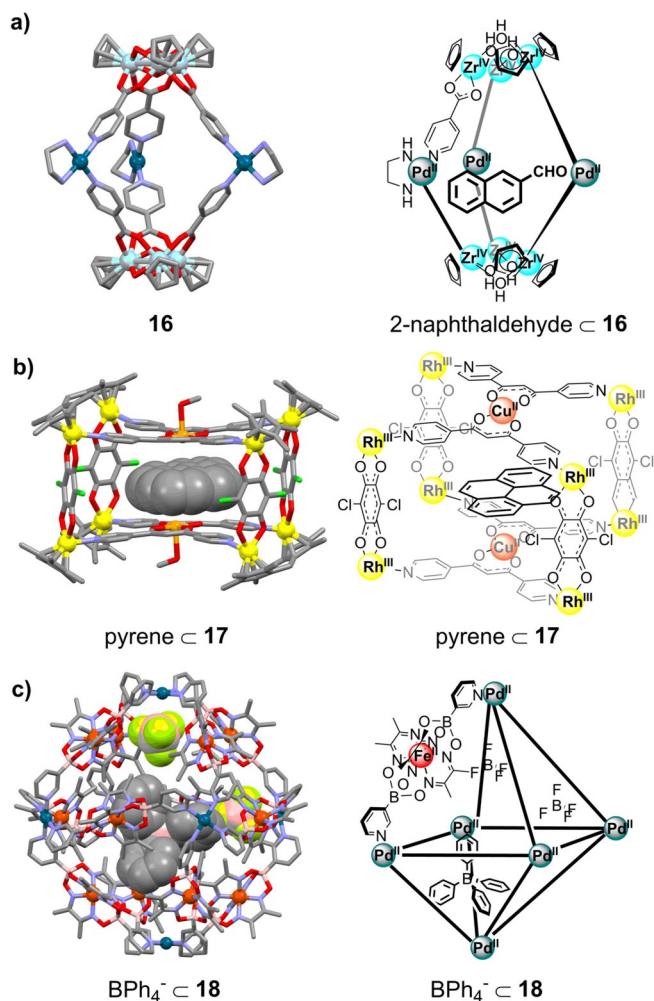


Figure 2. X-ray crystal structures of a) Zr₆Pd₃ trigonal bipyramid **16**;^[41] b) host-guest complex of pyrene \subset **17**;^[42] c) octahedral host-guest complex of **18** with three encapsulated BF₄⁻ ions and one BPh₄⁻ anion;^[47] (guest molecules are shown as space-fill models; hydrogen atoms, non-coordinated solvent molecules and non-encapsulated counter anions are omitted for clarity; color code: light blue—zirconium, petrol—palladium, yellow—rhodium, orange—copper, red—iron, blue—nitrogen, bright red—oxygen, green—chlorine, green-yellow—fluorine, beige—boron, grey—carbon).

ing out the importance of the hydrophobic effect in such host-guest systems.

These examples show that heterobimetallic cages can feature inner voids that are able to readily encapsulate neutral organic or anionic guest molecules.

Another interesting host-guest complex involving a heterobimetallic host was reported by Ward and co-workers. By using symmetric ligands with two pyrazole-pyridyl termini they reported on the formation of an inert metalloligand by coordinating one end of the ligand to Ru^{II} cations. This metalloligand can subsequently be used to assemble heterobimetallic^[26] and even mixed-metal, mixed-ligand coordination cages.^[48] After assembling the cubic Ru₄Co₄L₁₂ **20** framework, starting from ligand **19**, they found that this cage contains an additional [Na(BF₄)₄]³⁻ complex after crystallization over several months, with the sodium cation probably leached from the glassware. The four tetrafluoroborate anions assemble in a tetrahedral

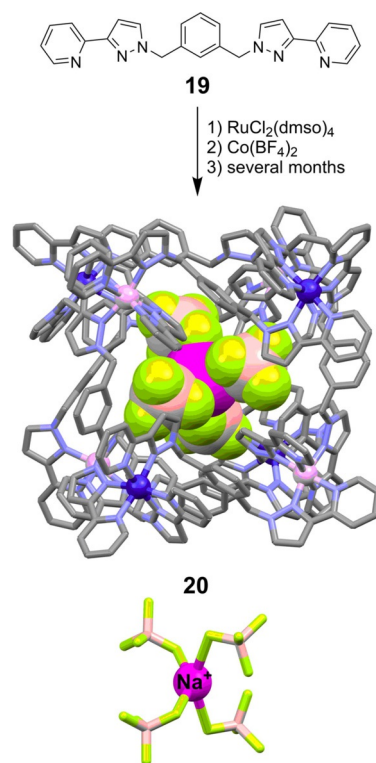
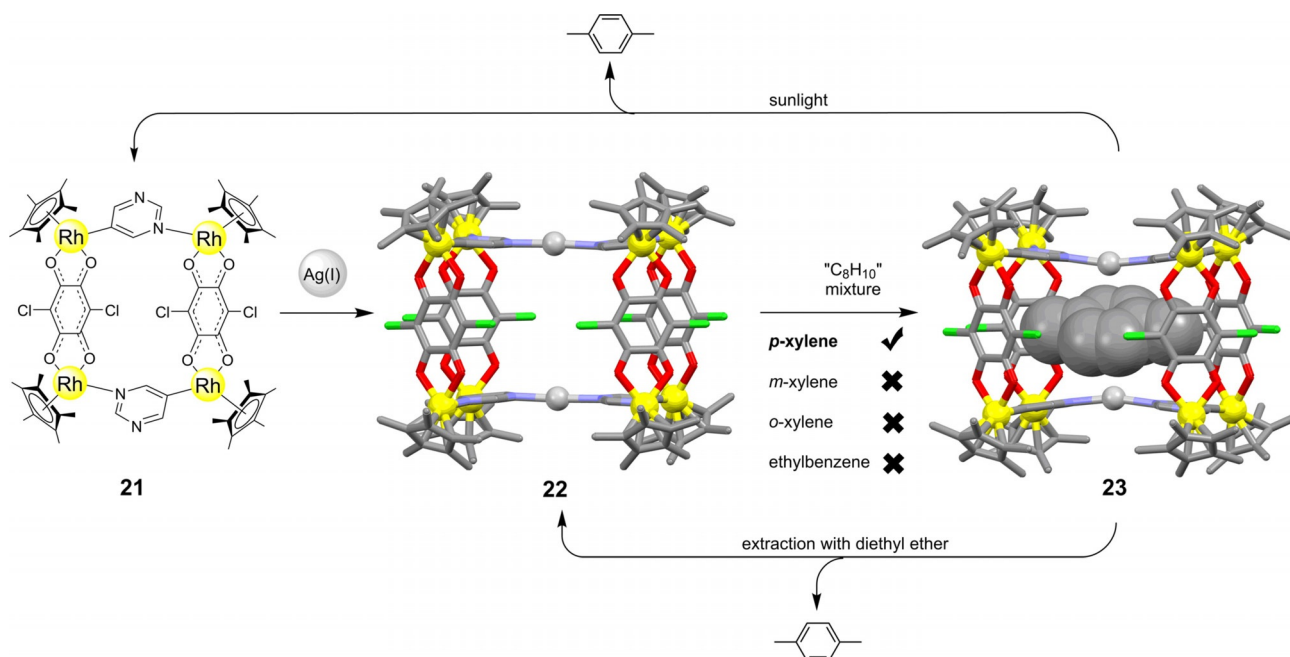


Figure 3. Ligand **19** can be used to form cage **20** in a stepwise assembly. Cage **20** was found to encapsulate an additional [Na(BF₄)₄]³⁻ complex (color code: purple—cobalt, light pink—ruthenium, pink—sodium, light green—fluorine, beige—boron, blue—nitrogen, grey—carbon).^[48]

fashion, each anion facing towards a Co^{II} site, creating a cavity in the cavity (Figure 3).

When it comes to heterobimetallic cages with additional functionality, the interplay between the different metal cations is not only of major importance for the construction of the cage itself, but also the different metal cations often adopt certain tasks to achieve a certain functionality.

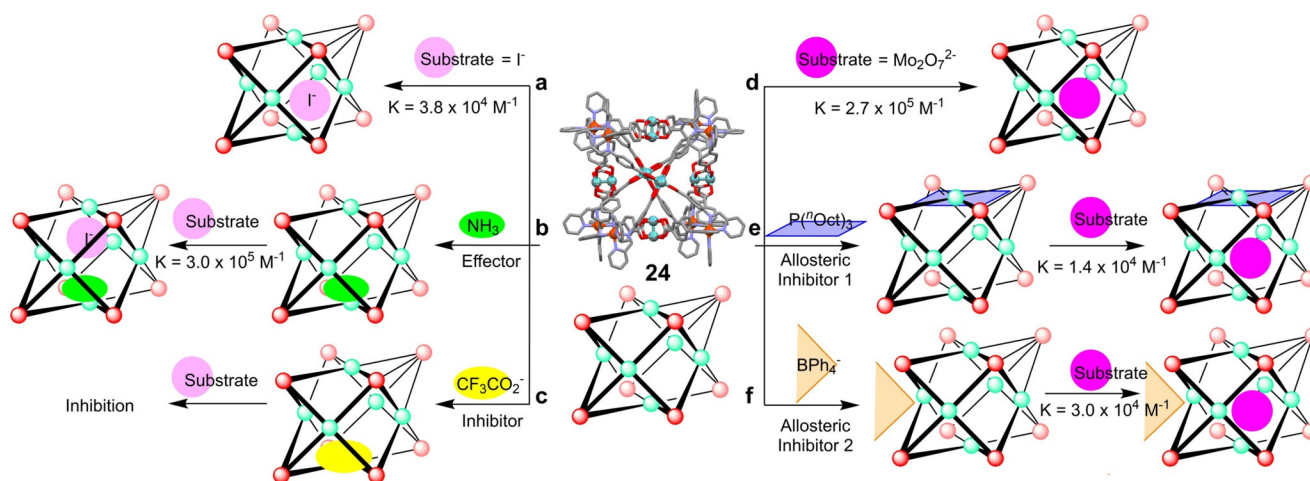
Jin and co-workers presented the box-like cage **22**, in which two silver(I) cations connect two tetranuclear [Rh₄] pyramidal frustums **21** (Scheme 3).^[49] They found that this capsule shows a high tendency for the encapsulation of *para*-substituted aromatic compounds, such as *p*-xylene, *p*-dichloro-, *p*-dibromo- and *p*-diiodobenzene. Crucial for these binding events was both, the size and shape matching as well as attractive Ag- π interactions. The selectivity for *p*-substituted aromatics was so high, that the capsule **22** could be used to separate *p*-xylene efficiently from its constitutional isomers from an equimolar mixture. The capsule was also able to separate *p*-dibromobenzene in the presence of excess *m*- and *o*-dibromobenzene. In case of *p*-xylene the encapsulated guest could be liberated by simple extraction with diethyl ether, recovering the intact capsule **22**. For other guests, the guest molecules could be released, when the host-guest complex was exposed to sunlight, yielding the free guests and metalloligand **21**. The interplay between structure determining Rh^{III} cations and connecting, as well as coordinating Ag^I cations facilitated the otherwise very difficult separation of the regioisomeric guest species.



Scheme 3. [Rh₄]-fragment **21** could be used as a metalloligand for the assembly of heterobimetallic **22**, which again could be used to separate *p*-xylene from its aromatic constitution isomers. Guest release was achieved either by extraction with diethyl ether or by exposure to sunlight. Color code: yellow—rhenium, silver—silver, green—chlorine, bright red—oxygen, blue—nitrogen, grey—carbon.^[49]

The controlled regulation of substrate binding events, like it can be found in many biological systems, requires communication between constituents of such networks.^[50] In artificial systems this is often achieved by the utilization of allosteric effects.^[51,52] In 2013 Nitschke and co-workers reported on a heterobimetallic cubic coordination cage based on a C₄ symmetric molybdenum(II) 'paddle-wheel' metalloligand.^[53] Combination of this metalloligand with pyridine-2-carbaldehyde and iron(II) cations yielded the cage **24** that was found to be able to encapsulate one iodide anion with a binding constant of $3.8 \times 10^4 \text{ M}^{-1}$ (Scheme 4 path a). However, the strength of this binding event could be manipulated by different small molecules.

24 could also encapsulate up to six ammonia molecules, which bind to the molybdenum moieties inside the cavity. Ammonia appeared to be an effector for the iodide binding, since the binding of I⁻ was eight times stronger in the presence of ammonia (Scheme 4 path b). This might be a result of decreased Coulomb interactions between iodide and weakly coordinating triflate from **24**, which was replaced by ammonia inside the cavity and also additional hydrogen-bonds between NH₃ and I⁻ might enhance the binding of iodide. The presence of CF₃CO₂⁻ on the other hand inhibited the iodide uptake and therefore could be used as an inhibitor, most likely based on unfavorable Coulomb interactions (Scheme 4 path c).



Scheme 4. Allosteric regulation of guest binding properties of heterobimetallic cube **24** (color code: red—iron, light green—molybdenum, bright red—oxygen, blue—nitrogen, grey—carbon).^[53,54]

This study was extended one year later, when two distinct allosteric sites were described on the very same cage.^[54] The substrate in this work was $\text{Mo}_2\text{O}_7^{2-}$, which was encapsulated by **24** with a binding constant of $2.7 \times 10^5 \text{ M}^{-1}$ (Scheme 4 path d). Tri-*n*-octylphosphine could bind to the molybdenum moieties from outside the cavity and thereby decrease the binding constant for the uptake of $\text{Mo}_2\text{O}_7^{2-}$ to $1.4 \times 10^4 \text{ M}^{-1}$, most likely based on the *trans* effect across the Mo_2 units (Scheme 4 path e). Tetraphenylborate on the other hand could bind to one edge of **24**, probably based on edge-to-face interactions, also inhibiting the encapsulation of $\text{Mo}_2\text{O}_7^{2-}$ because of unfavorable electrostatic repulsion between the inhibitor and the guest (Scheme 4 path f). However, the presence of BPh_4^- did not affect the binding of $\text{P}(n\text{Oct})_3$ and therefore both inhibitors could be used independently from each other to regulate the guest uptake.

In a following study Nitschke and co-workers could also show that subtle ligand modifications could invert the halide binding hierarchy in such cubic cages.^[55]

These examples impressively show how two different metal cations in one coordination cage can complement one another by adopting different tasks, like determining the cage (and cavity) geometry and offering additional binding motifs for small molecules or ions.

Magnetic properties

Connecting several metal centers with unpaired electrons in metallosupramolecular assemblies might lead to materials that exhibit interesting and exciting magnetic properties. Connecting two different metal cations might also lead to unusual magnetic communication between both types of metals and there already is a number of examples for heterobimetallic cages that feature interesting magnetic behavior.

In 2015 Wang and co-workers introduced a chiral organic ligand that self-assembles into heterobimetallic cubic cages with zinc(II) and palladium(II) cations. Interestingly, the chirality of the ligand controlled the resulting chirality of the stereogenic zinc cations, presenting the first diastereoselective synthesis of enantiomerically pure *O* symmetric cages.^[56] This purely diamagnetic system was expanded in 2018, when the very same ligand was used in combination with metal cations that feature unpaired electrons to assemble M_8Cu_6 cubic cages ($\text{M} = \text{Ni}^{\text{II}} = \mathbf{25}$, $\text{M} = \text{Co}^{\text{II}} = \mathbf{26}$) (Figure 4).^[57] Magnetic measurements with these cages revealed, that the data for **25** obey the Curie–Weiss law with $C = 12.45 \text{ cm}^3 \text{ mol}^{-1} \text{ K}$ and $\theta = -1.37 \text{ K}$, which suggests weak antiferromagnetic interactions between the metal cations. However, for **26** the data deviate from the Curie–Weiss law at around 45 K, probably due to spin-orbit coupling of the Co^{II} ions, which might be the main contribution to the magnetic behavior, besides weak antiferromagnetic coupling (Figure 4a and b).

Using 1-(4-pyridyl)butane-1,3-dione as an organic ligand, Brechin and co-workers developed a series of heterobimetallic cubic cages with metal compositions following $[\text{M}^{\text{III}}_8\text{M}^{\text{II}}_6]$, where M^{III} is Cr^{3+} or Fe^{3+} and M^{II} is Pd^{2+} , Co^{2+} , Ni^{2+} or Cu^{2+} .^[58,59] Most of these assemblies showed weak intermetallic

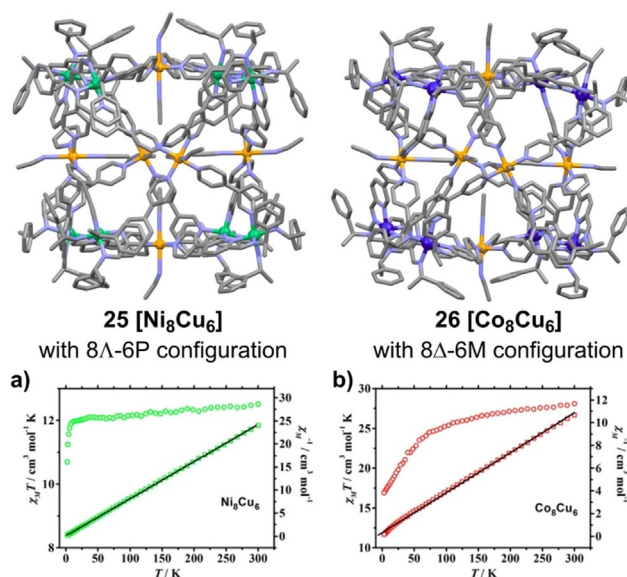


Figure 4. X-ray crystal structures of enantiomerically pure **25** and **26** (top) (color code: orange—copper, greenish—nickel, purple—cobalt, blue—nitrogen, grey—carbon). Plot of $\chi_M T$ vs. T (left axis), χ_M^{-1} vs. T (right axis) and corresponding linear fit of (a) **25** and (b) **26** (adapted with permission from ref. [57], copyright 2018, American Chemical Society).

interactions: the $[\text{Cr}_8\text{Cu}_6]$ coordination cube, e.g., showed weak ferromagnetic coupling while the magnetic behavior of $[\text{Cr}_8\text{Co}_6]$ was dominated by the axial ligand field splitting of Co^{2+} .^[58]

The magnetic data for $[\text{Fe}_8\text{Cu}_6]$ **27**, $[\text{Fe}_8\text{Ni}_6]$ **28** and $[\text{Fe}_8\text{Co}_6]$ **29** are given in Figure 5. For **27** and **28** the magnetic susceptibility essentially follows the Curie law down to 50 K, where the susceptibility drops rapidly. However, for **29** the deviation from the Curie law already starts at 180 K, before decreasing abruptly at 15 K. In all of these cases this behavior probably results from weak antiferromagnetic interactions between the paramagnetic metal cations and additional zero-field splitting in case of **28** and **29**. Using EPR spectroscopy it could also be shown, that the zero-field splitting of iron(III) cations within the heterobimetallic networks is larger, than in the mononuclear metalloligand, showing how the properties of the metal ions can be tuned by assembling heterobimetallic structures.^[59] Very similar results were obtained, when trigonal bipyramidal cages from the same organic ligand were investigated,^[60] showing that this system provides high flexibility with regard to the cage structure and the choice of the metal cations.

In 2016 the group of Li presented the first 3d–4f heterobimetallic coordination cage, containing Dy^{III} and Cu^{II} cations.^[61] The use of a non-centrosymmetric metalloligand resulted in the formation of the slightly distorted square prismatic $[\text{Dy}_8\text{Cu}_6]$ box **30**. As dysprosium(III) is known to often exhibit interesting magnetic behavior, like magnetic bistability in single-molecule-magnets,^[62] the potential communication between Dy^{III} and Cu^{II} in **30** was of special interest. Figure 6a shows the χT vs. T plot of **30**, which is nearly constant above 100 K, with an effective magnetic moment of $29.6 \mu_B$, which is consistent with eight Dy^{III} with $S = 5/2$ and six Cu^{II} with $S = 1/2$.

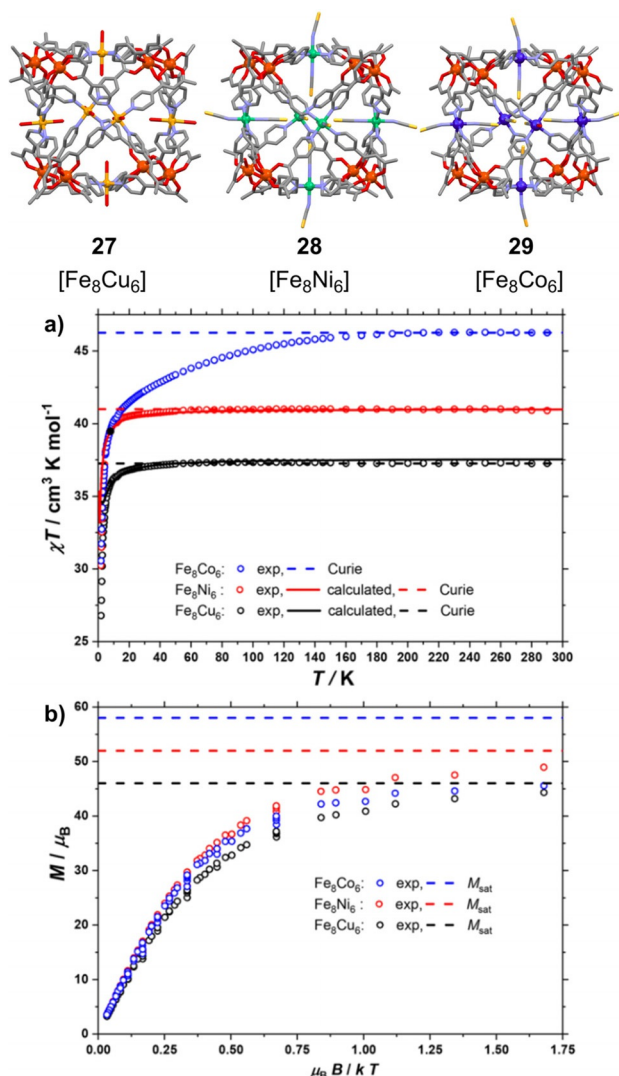


Figure 5. Solid state structures of **27**, **28**, and **29** (top) (color code: red—iron, orange—copper, greenish—nickel, purple—cobalt, bright red—oxygen, blue—nitrogen, yellow—sulfur, grey—carbon). a) Plot of χT vs. T for **27–29** ($B = 0.1 \text{ T}$) (solid lines are a fit of the experimental data, dashed lines are the Curie constants). b) Magnetization of **27–29** in field ranges of $T = 2\text{--}7 \text{ K}$ and $B = 0\text{--}7 \text{ T}$ (dashed lines indicate the saturation values expected for the field-induced alignment of all isotropic spin centers) (reprinted with permission from ref. [59], copyright 2018, American Chemical Society).

Below 100 K the behavior is dominated by zero-field splitting, with a minimum at 11 K, after which χT increases rapidly, indicating ferromagnetic coupling between Dy^{III} and Cu^{II} . The zero-field splitting and ferromagnetic coupling suggested single-molecule-magnet behavior for **30**. Indeed, the out-of-phase AC magnetic susceptibility χ'' (Figure 6b) showed a characteristic frequency dependency and slow magnetic relaxation, as expected for weak single-molecule-magnets. Similar results could also be found with $[\text{Fe}^{\text{III}}\text{Cu}^{\text{II}}_6]$ cages.^[63] Hence, using of non-centrosymmetric metalloligands like in **30** might be a way to increase the overall anisotropy of magnetic cages and provides a new approach to ‘tune’ the coordination sphere of magnetic metal cations.

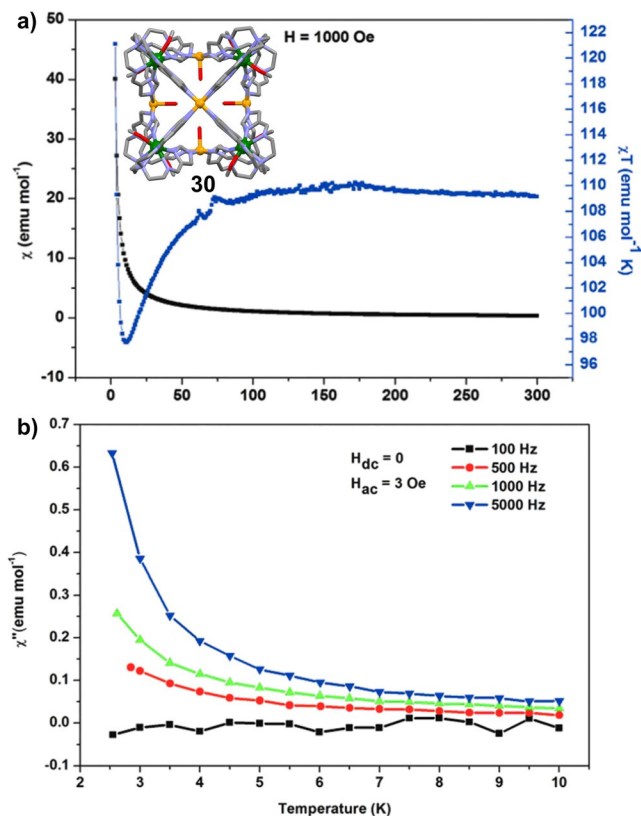


Figure 6. Solid state structure of $[\text{Dy}_8\text{Cu}_6]$ **30** (color code: dark green—dysprosium, orange—copper, red—oxygen, blue—nitrogen, grey—carbon). (a) Magnetic susceptibility χ and χT vs. T . (b) Temperature dependence of the out-of-phase components of the AC susceptibility for frequencies of 100–5000 kHz (reproduced with permission from ref. [61], copyright 2016, Royal Society of Chemistry)

Besides the described magnetic behaviors, another magnetic phenomenon of major interest is the spin-crossover process, in which metal centres can switch their spin state from low- to high-spin (and vice versa) upon a certain external stimulus, like temperature, light or pressure.^[64] In the past few years a growing number of metallocages was investigated, as they offer the possibility to mechanically connect spin-crossover centers.^[65]

Frequently used and notably versatile building blocks for the assembly of heterobimetallic cages are metallaporphyrins, as they give access to various geometries and functions.^[66] These cages often show very interesting host–guest behavior towards aromatic guests^[67–69] and can even exhibit antiaromatic character.^[70]

However, these building blocks also proved useful for the design of cages with interesting magnetic properties. In 2011 the Nitschke group presented a heterobimetallic cubic system based on a porphyrin backbone and the metal composition $[\text{Fe}^{\text{II}}_8\text{M}^{\text{II}}_6]$ ($\text{M}^{\text{II}} = \text{Ni}^{2+}, \text{Zn}^{2+}$) that facilitated the encapsulation of large aromatic guests, such as coronene, C_{60} and C_{70} .^[71] In 2017 the porphyrin-based ligand system could be modified in our group, so that the $[\text{Fe}_8\text{Zn}_6]$ cube **31** could be obtained, with coordinating tris(imidazolylimine) moieties.^[72] The iron(II) cations in this coordination sphere exhibit spin-crossover behav-

ior, which could be investigated in solution, using the Evans' method and the ideal solution model (Figure 7). The spin-crossover of **31** was located at $T_{1/2} = 247.7$ K. Interestingly, the encapsulation of C_{70} as a guest in **31** resulted in the stabilization of the high-spin state and decreased the transition temperature by 11 K. According to thermodynamic data from the ideal solution model, this was a consequence of an increased transition entropy with the encapsulated guest molecule.

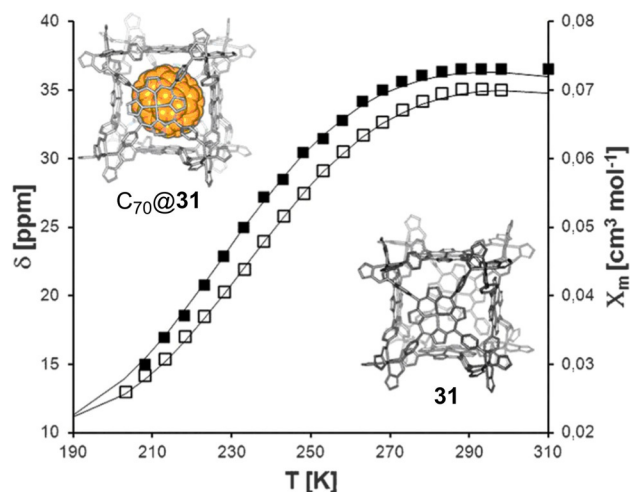


Figure 7. Chemical shifts of a selected proton in temperature-dependent ^1H -NMR experiments in $[\text{D}_4]\text{MeOH}$. Empty squares **31**, filled squares $C_{70}@31$, and calculated molar susceptibility χ_M based on the ideal solution model (black lines, scaled) (adapted from ref. [72], copyright 2017, Wiley-VCH).

Another example of a heterobimetallic spin-crossover assembly came from the group of Batten.^[73] Starting from a neutral Cu^I metalloligand, self-assembly with $\text{Fe}(\text{NCS})_2$ gave the heterobimetallic nanoball **32** that featured two crystallographically distinct iron(II) sites: $[\text{Fe}^{II}(\text{NCS})_2(\text{py})_4]$ and $[\text{Fe}^{II}(\text{NCS})(\text{CH}_3\text{CN})(\text{py})_4]$. The measurement of the magnetic susceptibility revealed that approximately half of the iron(II) centers switch from high- to low-spin upon cooling to 80 K. Below 10 K the measurement is affected by the zero-field splitting of high-spin states (Figure 8a). Mössbauer spectroscopy suggested, that the $[\text{Fe}^{II}(\text{NCS})(\text{CH}_3\text{CN})(\text{py})_4]$ sites undergo the spin-crossover process. Also, it was found that **32** undergoes light-induced switching by the light-induced excited spin state trapping effect (LIESST). Photomagnetic measurements at 10 K showed that irradiation with a green laser ($\lambda = 514.5$ nm) resulted in a rapid increase in χT from 1.6 to $3.4 \text{ cm}^3 \text{ mol}^{-1} \text{ K}$, proving the complete switching of low-spin species to a metastable high-spin state. The excited state can be 'erased' either by heating to 55 K, or by irradiation with a red laser ($\lambda = 830$ nm), inducing a reverse-LIESST effect. This on/off-switching was found to be a completely reversible process without observed diminishing (Figure 8b).

The presented magnetic materials beautifully show that two different metal cations can communicate within a heterobimetallic network, as long as the metal-to-metal distances are not too long. The use of magnetic metal cations may lead to mag-

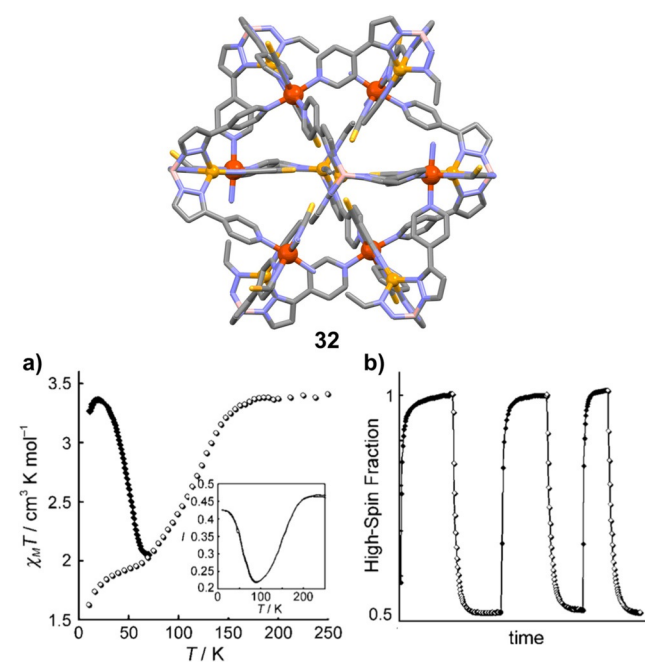


Figure 8. Solid state structure of nanoball **32** (top) (color code: red—iron, orange—copper, yellow—sulfur, blue—nitrogen, beige—boron, grey—carbon). (a) Plot of $\chi_M T$ vs. T per Fe^{II} ion (empty circles) and the light-induced excited metastable high-spin state with subsequent thermal relaxation (filled squares). (b) Cycling of green- (filled squares) and red- (empty squares) light-induced switching between high spin ('on') and low-spin ('off') states (adapted from ref. [73], copyright 2009, Wiley-VCH).

netic coupling, single-molecule magnets or spin-crossover compounds.

Photophysical properties

Transition metal cations and also organic chromophores can be used to equip metallocages with interesting photophysical properties. Here, the assembly of heterobimetallic structures could lead to exciting communication between the building blocks, in terms of energy transfer between metals and ligands and also metal-to-metal transfers. Beves and coworkers reported on a series of enantiopure, mononuclear ruthenium(II) complexes that showed luminescence and long excited-state lifetimes. These complexes could be used as metalloligands with cadmium(II) cations in order to assemble a one dimensional coordination polymer.^[74] Also, they could use a ruthenium(II)-containing metalloligand to construct heterobimetallic tetrahedra with iron(II) or zinc(II) cations. The photophysical properties of the metalloligand and heterobimetallic cages remained nearly identical, showing the potential for such inert ruthenium units in the construction of photoactive nanocages.^[75]

Using a symmetric ligand with a naphthalene core and a stepwise assembly strategy, Ward and coworkers reported on a $[\text{Os}_4\text{Cd}_4]$ cubic cage that featured both, redox- and photoactivity of the Os sites.^[76] Interestingly, the fluorescence characteristics of the naphthalene-containing ligand was completely quenched in this cage, indicating the presence of a (naph-

thyl)→Os^{II} energy transfer from the ligand to osmium(II) cations.

The group of Ribas presented cofacial zinc-porphyrin nanocapsules that were found to produce singlet oxygen (¹O₂) upon irradiation (Figure 9).^[77] The palladium(II)-based cage **33** showed a photosensitizing efficiency that was similar to Zn-tetraphenylporphyrin, however, the photostability of **33** was significantly enhanced.

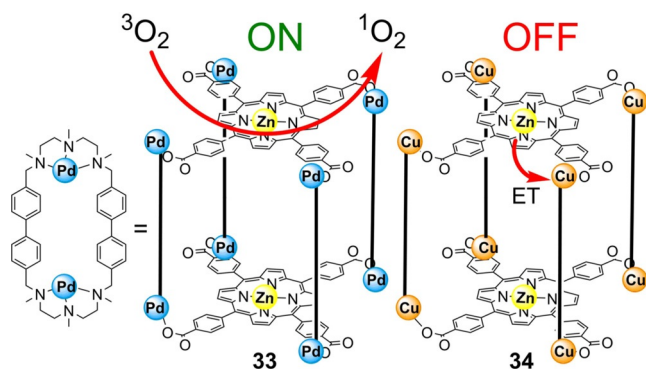


Figure 9. Palladium(II)-based **33** shows photosensitized ¹O₂-production upon irradiation with sun light (ON-state), whereas copper-based **34** is a dormant photosensitizer (OFF-state), because of the electron transfer (ET) from the zinc(II) porphyrin to copper(II) cations and can be switched 'on' by protonation.^[77]

Therefore, **33** proved to be useful as a robust catalyst for ¹O₂ production. On the other hand, the photosensitizing properties of copper(II)-based **34** were switched off, due to electron trans-

fer from the zinc-porphyrins to copper(II). Interestingly, **34** could be switched 'on' by protonation of the carboxylate groups, leading to disassembly of **34**. This process could also be reversed by deprotonation and subsequent re-assembly of the free building blocks to **34**. Thus, **34** could be used as a dormant photosensitizer that could be reversibly switched on/off by protonation/deprotonation cycles.

Another impressive luminescent cage came from the group of Sun.^[78] The chiral ligand **35** was used to form the mononuclear europium(III) complex **37** or the dinuclear palladium(II) metalloligand **36**, which could assemble the trigonal bipyramidal cage **38**, when combined with europium(III) cations (Figure 10a). Both, the mononuclear complex **37** and the heterobimetallic cage **38** showed luminescence upon excitation at 270 nm, with emissions featuring ⁵D₀→⁷F_J (*J*=1–4) transitions of Eu^{III}. However, the emission intensity at 615 nm of **38** was 40-fold higher than that observed with **37** (Figure 10b).

Luminescence titrations with the dipalladium metalloligand **36** revealed that the emission of Pd^{II} at 500 nm gradually diminished upon addition of Eu^{III}, with the red luminescence of Eu^{III} increasing simultaneously. This clearly indicates the effective energy transfer from the dinuclear palladium units to Eu^{III}, showing the beautiful interplay of the metal cations within this cage. Additionally, cage **38** proved useful as an antibiotic sensor, especially sensitive to penicillin G sodium salt (PCL-Na) as the presence of this antibiotic led to luminescence quenching. Since the quenching was linearly proportional to the PCL-Na concentration and the detection limit was only 2.177 × 10⁻⁸ M, **38** would be suitable as a quantitative PCL-Na sensor (Figure 10c).

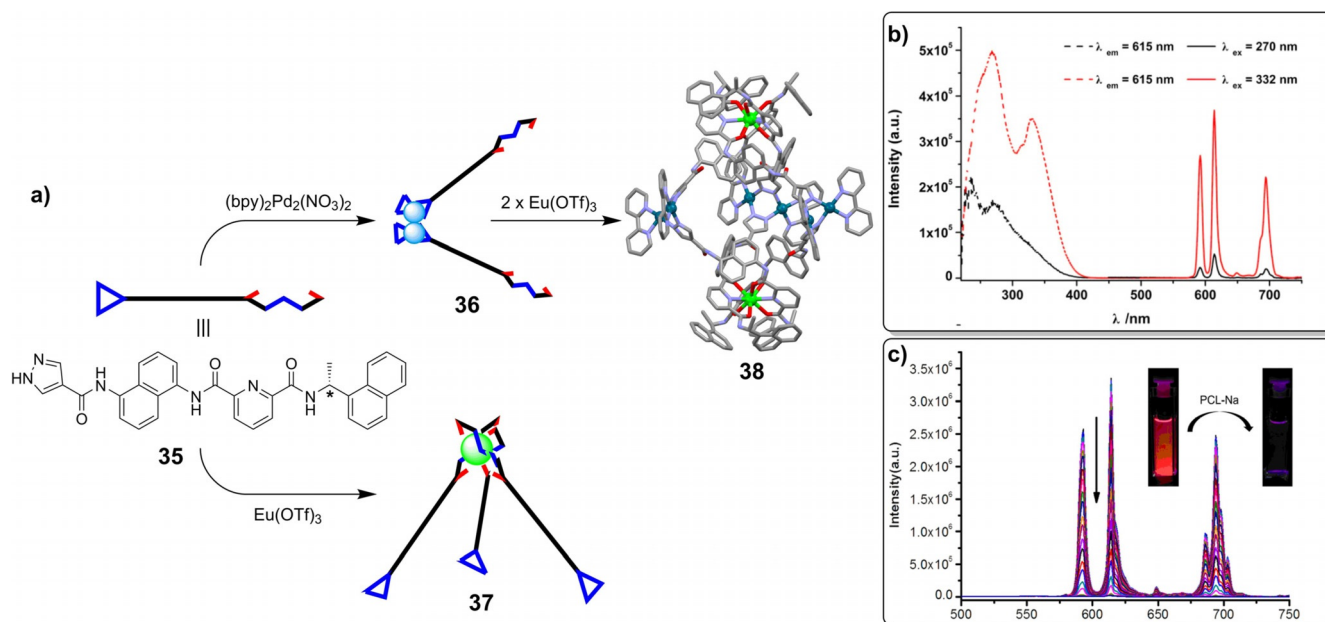
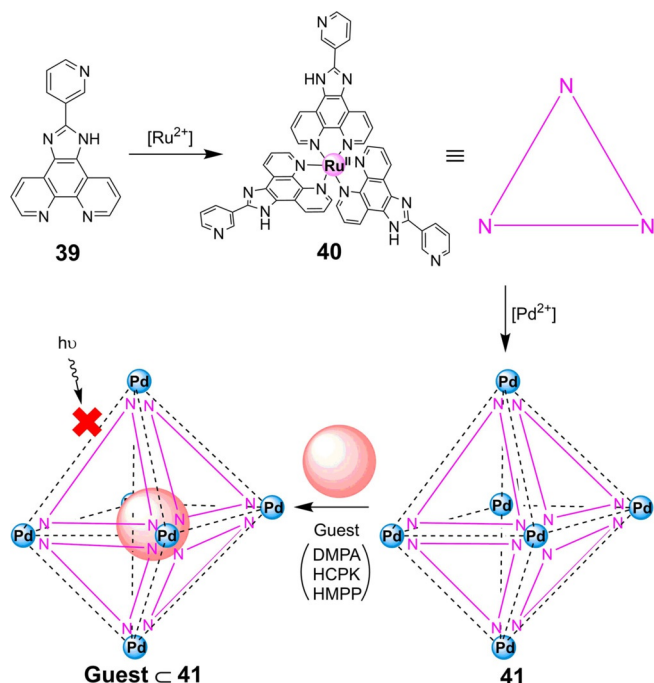


Figure 10. (a) Stepwise assembly and structure of **38** as determined by XRD analysis (hydrogen atoms, solvate and counter anions are omitted in the crystal structure; color code: petrol—palladium, green—europium, red—oxygen, blue—nitrogen, grey—carbon). (b) Excitation (dashed lines) and emission (solid lines) spectra of **37** (black, 3.33 × 10⁻⁶ M) and **38** (red, 1.67 × 10⁻⁶ M) (excitation and emission intensity of **37** is 10 times amplified for clarity). (c) Luminescence emission spectra (λ_{ex} = 345 nm) of **38** (20 μM) with the addition of 0–120 μM of PCL-Na. Inset shows photographs before and after the addition of PCL-Na (adapted with permission from ref. [78], copyright 2018, American Chemical Society).

The group of Su presented ruthenium-based cage **41** that assembled to a truncated octahedron with Pd^{II} cations.^[79] This cage features interesting optoelectrical properties while tolerating aqueous solutions and provides a large, hydrophobic cavity for the effective encapsulation of guest molecules (Scheme 5). Indeed, the heterobimetallic cage **41** was found to



Scheme 5. Stepwise assembly of the [Ru₆Pd₆] truncated octahedron **41**, capable of guest encapsulation.^[79]

be able for the uptake of aromatic, water insoluble guests, such as naphthalene, pyrene or anthracene in aqueous media, most likely favored by the hydrophobic effect. More fascinating, **41** also trapped the polar guests 2,2-dimethoxy-2-phenylacetophenone (DMPA), 1-hydroxycyclohexyl phenyl ketone (HCPK) and 2-hydroxy-2-methylpropiophenone (HMPP), molecules that are widely used in ink and paint, due to their photosensitive behavior. UV irradiation studies revealed a notable protective effect of cage **41** on the encapsulated photoinitiators. Although the mononuclear metalloligand **40** also shields these molecules, photolysis with **40** appeared after 24 h of irradiation, while the heterobimetallic cage **41** protected the photolabile guest molecules in aqueous solution up to 120 hours. This again shows how both metal cations within a heterobimetallic cage are of major importance to achieve certain and enhanced functionality and activity.

Redox activity

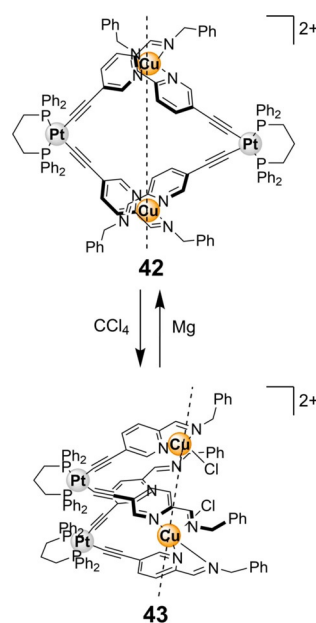
The incorporation of redox-active metal cations into supramolecular assemblies can lead to useful electrochemical properties. Besides the change of the overall charge of the complex, the change of the oxidation number is often connected with a change of the preferred coordination number and/or

geometry. Therefore, an overall modification of the complex structure might be achieved.

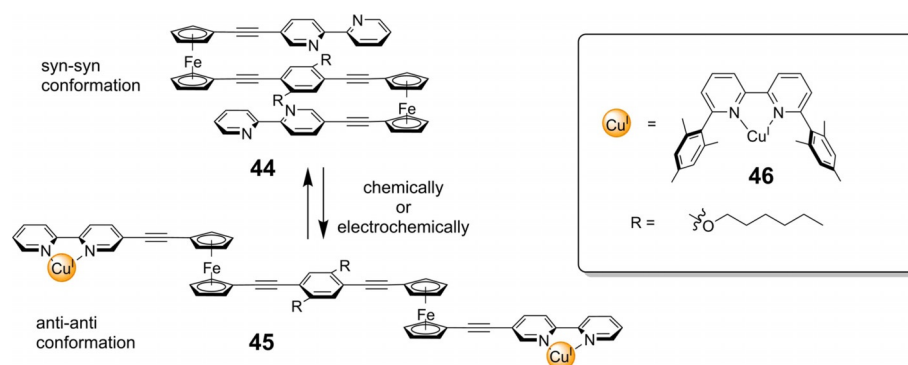
This Minireview already discussed Ward's [Os₄Cd₄] heterobimetallic cube that showed reversible redox behavior of the Os-sites.^[76] In an earlier study the same group could already present an analogous [Ru₄Cd₄] cage that exhibited redox activity, specifically at the Ru-sites^[80] and the group of Hanan reported on a [Ru₃Pd₃] triangle that undergoes quasi-reversible redox behavior with independently operating Ru-centers.^[81]

Severin and co-workers reported on the heterobimetallic [Pt₂Cu₂] macrocycle **42**, in which the Cu^I cations were found to undergo oxidation (Scheme 6). In this complex, the Cu^I cations are coordinated in a tetrahedral fashion, resulting in a rectangular structure with a Pt–Pt distance of around 12 Å. However, treatment with chlorinated solvents resulted in the oxidation of Cu^I to Cu^{II}. This oxidation proceeds via an atom transfer radical reaction, involving a homolytic cleavage of a carbon–chlorine bond. The abstracted chlorine atom is then found as a new chloride ligand coordinated to copper(II). The oxidation rate is dependent on the nature of the chlorinated solvent in accordance with the relative homolytic dissociation energies of the C–Cl bonds. Therefore, the oxidation proceeds fastest in CCl₄. The oxidation of Cu^I to Cu^{II} resulted in a change of the coordination geometry from tetrahedral to trigonal bipyramidal, which caused a major change in the complex structure. The rectangular complex **42** underwent a hinge motion along the Cu–Cu axis to build the butterfly-shaped complex **43** with a reduced Pt–Pt distance of 7.84 Å. The reverse reaction was possible, when **43** was treated with activated Mg, resulting in the recovery of **42**.^[82]

A frequently used redox-active building block for the construction of heterobimetallic assemblies is ferrocene.^[83–86] There is a study where ferrocene containing platinum(II) metallacy-



Scheme 6. Oxidation of **42** to **43** with CCl₄, coupled with a hinge motion. Reverse reaction proceeded via treatment with activated Mg.^[82]



Scheme 7. Chemical and electrochemical switching between folded **44** and unfolded **45** upon addition or removal of Cu^{I} moieties.^[91]

cles could even interact with so-called carbon dots (10 nm-sized carbon nanoparticles).^[87]

An interesting alternative use of ferrocene, despite its redox activity, is its use as a rotatable element for the construction of molecular machines. Following this approach, the group of Crowley could report on some switchable ferrocene-based rotors.^[88–90] The folded bis(ferrocene) **44** adopts a *syn-syn* conformation regarding the ferrocene moieties, with π - π interactions between pyridyl- and phenyl rings stabilizing the overall sandwich-like arrangement (Scheme 7).^[91] However, addition of copper(I) 6,6'-dimesityl-2,2'-bipyridine complex **46** resulted in a conformational change from folded **44** to unfolded *anti-anti* **45**. **46** was chosen in order to achieve the selective formation of heteroleptic complexes. The change to the *anti-anti* rotamer is most likely a result of steric and electrostatic repulsion between the copper complex fragments. The chemical reversal of this process was achieved by the addition of two equivalents of 1,4,8,11-tetraazacyclotetradecan (cyclam), with quantitative formation of Cu^{II} -cyclam and recovery of **44**. Addition of $[\text{Cu}(\text{CH}_3\text{CN})_4](\text{PF}_6)$ reformed **45** again, resulting in a completely reversible process. However, this switching produced huge amounts of waste products. A much cleaner switching was achieved electrochemically in CV experiments and even in bulk electrolysis in the presence of 2,2',6',2''-terpyridine (terpy). Starting from **45**, oxidation gave **44** and the formation of pentacoordinated $[\text{46}(\text{terpy})]$. Subsequent reduction reformed **45** with free terpy. This behavior is based on the preference for different coordination numbers of Cu^{I} (CN=4) and Cu^{II} (CN=5). This way, the redox activity within this system could be used in order to achieve a controlled molecular rotation.

Molecular flasks

An impressive application of metallosupramolecular cages is the use as molecular flasks or even supramolecular catalysts.^[92] Mimicking a main function of enzymes, such applications are of major interest, but likewise difficult to achieve. Still, there are some fascinating examples of heterobimetallic cages that are capable of mediating organic reactions within their cavities.^[93]

In 2013 the de Bruin group reported on a heterobimetallic cage that could be used as a molecular flasks for the catalysis

of radical-type reactions.^[94] The cubic cage **47** with porphyrin capped surfaces encapsulated 4-pyridyl substituted porphyrin guests, such as **48** with a central Co^{II} cation. Here, the 4-pyridyl donors of **48** coordinated to Zn^{II} cations, occupying the centers of the cube's faces. The Co^{II} cation in the center of the cubic assembly **49** was then found to be catalytically active towards diazo compounds in radical-type reactions. For example, the diazo ester **50** could enter the cage's cavity and was activated by the Co^{II} porphyrin to yield the carbon centered radical **52**.

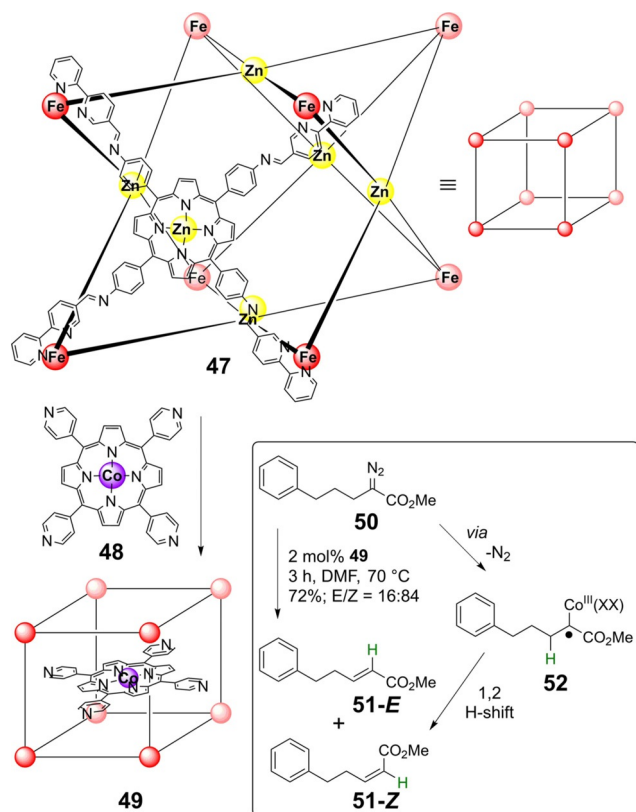
Unlike with similar compounds that were found to undergo a radical addition to the arene,^[95] intermediate **52** underwent a 1,2-hydrogen atom shift to yield the olefins **51** in 72% yield and with a notable diastereoselectivity of d.r. (*E/Z*)=16:84 (Scheme 8). The control reaction using **48** without cage **47** yielded less than 7% yield, pointing out the important role of the heterobimetallic cage.

The incorporation of Co^{II} -porphyrins into heterobimetallic molecular flasks was also investigated by Cook and co-workers in oxygen reduction catalysis in a $[\text{Ru}_8(\text{Co}^{\text{II}}\text{-porphyrin})_2]$ prism.^[96] The group of Reek reported on the photocatalytic production of molecular hydrogen by an artificial $[\text{FeFe}]$ hydrogenase that was encapsulated in a porphyrin-based capsule.^[97]

The group of Jin used Cp^* -capped Ir-moieties to construct heterobimetallic boxes together with Cu^{II} , Ni^{II} or Zn^{II} ions. The Lewis acidity of copper(II) cations within the heterobimetallic framework was further increased, due to the electron-withdrawing effect of the Cp^*Ir groups, exhibiting an increased activity in Lewis acid assisted reactions, such as the acetalization of aldehydes.^[98]

The group of Mukherjee reported on a molecular tube with eight Pd(dppf) (dppf = 1,1'-bis(diphenylphosphino)ferrocene) building blocks that was utilized to perform intramolecular cycloadditions of *O*-allylated benzylidenebarbituric acids in a regio- and stereoselective manner.^[99]

Su and co-workers reported on the application of the octahedral cage **41**, that was already introduced as a protecting cage for photolabile molecules in this Minireview earlier (vide supra, Scheme 5), as a molecular flask.^[100] Since **41** is photo- and redox-active and features a confined chiral cavity, its potential in photodimerizations within its homochiral cavity was



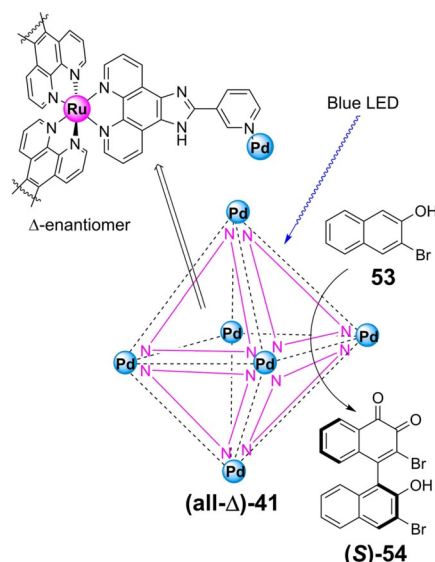
Scheme 8. Heterobimetallic cage **47** encapsulated guest **48** with a central Co^{II} cation, which could then be used to perform radical-type reactions.^[94]

investigated. Interestingly, the coupling of naphthols and their derivatives yielded the unusual 1,4-coupling products, instead of 1,1-couplings. It was found that irradiation with a blue LED was crucial to initiate the reaction, since no product was detected without light irradiation. Because of product inhibition, it was necessary to extract the product from the cage after the reaction, however, since it was found that cage **41** can encapsulate up to nine naphthol molecules, only 10 mol% of the cage were sufficient to perform the reaction. Conversion of **53** in the presence of 10 mol% of (*all-Δ*)-**41** in acetonitrile/water (1:1) upon irradiation with a blue LED yielded (*S*)-**54** in an overall yield of 32% and an *ee* of 32% after 24 hours at room temperature (Scheme 9). As the product was found to racemize in solution after extraction, the initial *ee* might even be higher. Additionally, homochiral cages **41** were found to protect the stereo information of the product, as racemization proceeded much slower inside the cavities. ESR spectroscopy indicated a radical mechanism, as superoxide, hydroxyl and naphthoxy radicals were detected during the photoreaction.

These examples might demonstrate the enormous potential of heterobimetallic cages that feature defined cavities to conduct organic reactions as molecular flasks.

Conclusion and Outlook

Metallo-supramolecular cages have been and continue to be of major interest in material science and nanotechnology for



Scheme 9. Enantiomerically pure **41** can transform **53** into **54** in a stereo- and regioselective manner upon irradiation with a blue LED.^[100]

about three decades now. Having learned much about the assembly, properties and functions of homometallic assemblies the development of heterometallic analogues is one of the obvious strategies to increase the structural and functional diversity of these fascinating (supra-)molecular architectures. Over the last years significant progress has been made to develop reliable design concepts to access heterobimetallic complexes with manifold compositions, geometries and sizes. Very often such structures even tolerate the use of a series of different metal cations with similar coordination preferences and charge densities, so that a whole series of complexes with different properties can be obtained from one single ligand.

As a result, more and more assemblies are described that incorporate more than one type of metal cation and feature certain functionalities that open the quest for applications.

Heterobimetallic assemblies combine the properties of two different metal cations within one discrete aggregate. This offers the unique chance to achieve enhanced or even entirely new properties through the interplay and communication of these metal cations, as shown in many examples in this Minireview.

We have focused on the discussion of recent examples for heterobimetallic assemblies with interesting dynamic structural behavior, their host–guest chemistry, their magnetic and photophysical properties, their redox-activities and their use as molecular flasks, thus, giving a glimpse of the huge potential of these metallosupramolecular architectures.

However, there are also additional and more specialized functionalities known in heterobimetallic systems. Mukherjee and co-workers, for example, presented heterobimetallic assemblies that show high proton conductivity, based on coordinated water molecules as proton sources and guest water molecules as proton conducting pathways.^[101] The group of Schmittel reported on heterobimetallic high-speed rotors, based on a zinc-porphyrin platform.^[102,103] Chi and co-workers

even reported on heterobimetallic rectangles with anticancer activity.^[104]

The presented properties and functions may lead to various applications of heterobimetallic assemblies in the future. Dynamic systems may be used to access smart switches that undergo major structural changes upon chemical stimuli. That way, for example, the triggered encapsulation and release of guest molecules might be controlled, even in complex multi-component systems. The large and often easy to achieve variety of cage sizes and properties allows for a fine-tuning of guest binding properties, for example, useful for the effective separation of constitutional or even stereoisomers that otherwise would be very difficult or even impossible. Potential magnetic communication between two different metal cations may give access to new single molecule magnets and spin-cross-over compounds, which are highly interesting for potential applications in quantum computing or the development of new nanosized storage media and switches. Communication in heterobimetallic photo- or redoxactive compounds may be very useful in terms of sensing, energy transfers or the construction of sophisticated molecular motors. Molecular flasks that are assembled from two different metal cations might lead to enhanced or entirely new reactivity, new ways to control reaction pathways and offer the chance to combine two catalytically active metal cations within one discrete assembly.

All these examples beautifully show how the field of heterobimetallic assemblies is growing and will continue to do so in the future and how it constantly expands to explore new areas. Being still in its infancy we are looking forward for the new developments in this field ahead of us—certainly, the best is still to come.

Acknowledgements

M.H. thanks the Jürgen Manchot Foundation for a doctoral scholarship.

Conflict of interest

The authors declare no conflict of interest.

Keywords: functional materials · heterobimetallic complexes · metallosupramolecular cages · supramolecular catalysts · supramolecular chemistry

- [1] D. L. Caulder, K. N. Raymond, *J. Chem. Soc. Dalton Trans.* **1999**, 1185–1200.
- [2] B. Olenyuk, A. Fechtenkötter, P. J. Stang, *J. Chem. Soc. Dalton Trans.* **1998**, 1707–1728.
- [3] M. Fujita, *Chem. Soc. Rev.* **1998**, 27, 417.
- [4] R. Chakrabarty, P. S. Mukherjee, P. J. Stang, *Chem. Rev.* **2011**, 111, 6810–6918.
- [5] M. M. J. Smulders, I. A. Riddell, C. Browne, J. R. Nitschke, *Chem. Soc. Rev.* **2013**, 42, 1728–1754.
- [6] L. Chen, Q. Chen, M. Wu, F. Jiang, M. Hong, *Acc. Chem. Res.* **2015**, 48, 201–210.
- [7] C. J. Brown, F. D. Toste, R. G. Bergman, K. N. Raymond, *Chem. Rev.* **2015**, 115, 3012–3035.

- [8] T. R. Cook, P. J. Stang, *Chem. Rev.* **2015**, 115, 7001–7045.
- [9] Q. Yang, J. Tang, *Dalton Trans.* **2019**, 48, 769–778.
- [10] Y.-Y. Zhang, W.-X. Gao, L. Lin, G.-X. Jin, *Coord. Chem. Rev.* **2017**, 344, 323–344.
- [11] H. Li, Z.-J. Yao, D. Liu, G.-X. Jin, *Coord. Chem. Rev.* **2015**, 293–294, 139–157.
- [12] S. Hiraoka, Y. Sakata, M. Shionoya, *J. Am. Chem. Soc.* **2008**, 130, 10058–10059.
- [13] H. Sepehrpour, M. L. Saha, P. J. Stang, *J. Am. Chem. Soc.* **2017**, 139, 2553–2556.
- [14] D. Preston, R. A. J. Tucker, A. L. Garden, J. D. Crowley, *Inorg. Chem.* **2016**, 55, 8928–8934.
- [15] Y.-Y. Zhang, Y.-J. Lin, G.-X. Jin, *Chem. Commun.* **2014**, 50, 2327–2329.
- [16] Y. Sakata, S. Hiraoka, M. Shionoya, *Chem. Eur. J.* **2010**, 16, 3318–3325.
- [17] M. Albrecht, R. Fröhlich, *J. Am. Chem. Soc.* **1997**, 119, 1656–1661.
- [18] F. E. Hahn, M. Offermann, C. Schulze Isfort, T. Pape, R. Fröhlich, *Angew. Chem. Int. Ed.* **2008**, 47, 6794–6797; *Angew. Chem.* **2008**, 120, 6899–6902.
- [19] T. Kreickmann, F. E. Hahn, *Chem. Commun.* **2007**, 1111–1120.
- [20] S. M. Jansze, G. Cecot, M. D. Wise, K. O. Zhurov, T. K. Ronson, A. M. Castilla, A. Finelli, P. Pattison, E. Solari, R. Scopelliti, G. E. Zelinski, A. V. Volozhanina, Y. Z. Voloshin, J. R. Nitschke, K. Severin, *J. Am. Chem. Soc.* **2016**, 138, 2046–2054.
- [21] H.-B. Wu, Q.-M. Wang, *Angew. Chem. Int. Ed.* **2009**, 48, 7343–7345; *Angew. Chem.* **2009**, 121, 7479–7481.
- [22] M. Hardy, N. Struch, F. Topić, G. Schnakenburg, K. Rissanen, A. Lützen, *Inorg. Chem.* **2018**, 57, 3507–3515.
- [23] X. Sun, D. W. Johnson, D. L. Caulder, R. E. Powers, K. N. Raymond, E. H. Wong, *Angew. Chem. Int. Ed.* **1999**, 38, 1303–1307; *Angew. Chem.* **1999**, 111, 1386–1390.
- [24] F. Reichel, J. K. Clegg, K. Gloe, J. J. Weigand, J. K. Reynolds, C.-G. Li, J. R. Aldrich-Wright, C. J. Kepert, L. F. Lindoy, H.-C. Yao, F. Li, *Inorg. Chem.* **2014**, 53, 688–690.
- [25] A. A. Adeyemo, P. S. Mukherjee, *Beilstein J. Org. Chem.* **2018**, 14, 2242–2249.
- [26] A. J. Metherell, M. D. Ward, *Chem. Commun.* **2014**, 50, 10979–10982.
- [27] J. Y. Ryu, Y. J. Park, H.-R. Park, M. L. Saha, P. J. Stang, J. Lee, *J. Am. Chem. Soc.* **2015**, 137, 13018–13023.
- [28] M. L. Saha, J. W. Bats, M. Schmittel, *Org. Biomol. Chem.* **2013**, 11, 5592–5595.
- [29] M. L. Saha, N. Mittal, J. W. Bats, M. Schmittel, *Chem. Commun.* **2014**, 50, 12189–12192.
- [30] C. Giri, F. Topić, M. Cametti, K. Rissanen, *Chem. Sci.* **2015**, 6, 5712–5718.
- [31] S.-L. Huang, Y.-J. Lin, Z.-H. Li, G.-X. Jin, *Angew. Chem. Int. Ed.* **2014**, 53, 11218–11222; *Angew. Chem.* **2014**, 126, 11400–11404.
- [32] Y. Lu, Y.-J. Lin, Z.-H. Li, G.-X. Jin, *Chin. J. Chem.* **2018**, 36, 106–111.
- [33] H.-N. Zhang, W.-X. Gao, Y.-J. Lin, G.-X. Jin, *J. Am. Chem. Soc.* **2019**, 141, 16057–16063.
- [34] J. Park, Y.-P. Chen, Z. Perry, J.-R. Li, H.-C. Zhou, *J. Am. Chem. Soc.* **2014**, 136, 16895–16901.
- [35] J. R. Nitschke, *Acc. Chem. Res.* **2007**, 40, 103–112.
- [36] M. M. J. Smulders, A. Jiménez, J. R. Nitschke, *Angew. Chem. Int. Ed.* **2012**, 51, 6681–6685; *Angew. Chem.* **2012**, 124, 6785–6789.
- [37] M. Hardy, N. Struch, J. J. Holstein, G. Schnakenburg, N. Wagner, M. Engeser, J. Beck, G. H. Clever, A. Lützen, *Angew. Chem. Int. Ed.* **2020**, 59, 3195–3200; *Angew. Chem.* **2020**, 132, 3221–3226.
- [38] W. J. Ramsay, F. T. Szczypiński, H. Weissman, T. K. Ronson, M. M. J. Smulders, B. Rybtchinski, J. R. Nitschke, *Angew. Chem. Int. Ed.* **2015**, 54, 5636–5640; *Angew. Chem.* **2015**, 127, 5728–5732.
- [39] C. Colomban, V. Martin-Diaconescu, T. Parella, S. Goeb, C. García-Simón, J. Lloret-Fillol, M. Costas, X. Ribas, *Inorg. Chem.* **2018**, 57, 3529–3539.
- [40] J.-J. Liu, Y.-J. Lin, G.-X. Jin, *Organometallics* **2014**, 33, 1283–1290.
- [41] M. Maity, P. Howlader, P. S. Mukherjee, *Cryst. Growth Des.* **2018**, 18, 6956–6964.
- [42] Y.-Y. Zhang, L. Zhang, Y.-J. Lin, G.-X. Jin, *Chem. Eur. J.* **2015**, 21, 14893–14900.
- [43] Q.-J. Fan, Y.-J. Lin, F. E. Hahn, G.-X. Jin, *Dalton Trans.* **2018**, 47, 2240–2246.

- [44] W.-X. Gao, Q.-J. Fan, Y.-J. Lin, G.-X. Jin, *Chin. J. Chem.* **2018**, *36*, 594–598.
- [45] J. L. Bila, P. Pijeat, A. Ramorini, F. Fadaei-Tirani, R. Scopelliti, E. Baudat, K. Severin, *Dalton Trans.* **2019**, *48*, 4582–4588.
- [46] S. M. Jansze, K. Severin, *Acc. Chem. Res.* **2018**, *51*, 2139–2147.
- [47] M. D. Wise, J. J. Holstein, P. Pattison, C. Besnard, E. Solari, R. Scopelliti, G. Bricogne, K. Severin, *Chem. Sci.* **2015**, *6*, 1004–1010.
- [48] A. J. Metherell, M. D. Ward, *Chem. Sci.* **2016**, *7*, 910–915.
- [49] W.-Y. Zhang, Y.-J. Lin, Y.-F. Han, G.-X. Jin, *J. Am. Chem. Soc.* **2016**, *138*, 10700–10707.
- [50] D. Ray, J. T. Foy, R. P. Hughes, I. Aprahamian, *Nat. Chem.* **2012**, *4*, 757–762.
- [51] L. Kovbasyuk, R. Krämer, *Chem. Rev.* **2004**, *104*, 3161–3188.
- [52] C. Kremer, A. Lützen, *Chem. Eur. J.* **2013**, *19*, 6162–6196.
- [53] W. J. Ramsay, T. K. Ronson, J. K. Clegg, J. R. Nitschke, *Angew. Chem. Int. Ed.* **2013**, *52*, 13439–13443; *Angew. Chem.* **2013**, *125*, 13681–13685.
- [54] W. J. Ramsay, J. R. Nitschke, *J. Am. Chem. Soc.* **2014**, *136*, 7038–7043.
- [55] W. J. Ramsay, F. J. Rizzuto, T. K. Ronson, K. Caprice, J. R. Nitschke, *J. Am. Chem. Soc.* **2016**, *138*, 7264–7267.
- [56] Y. Yang, J.-H. Jia, X.-L. Pei, H. Zheng, Z.-A. Nan, Q.-M. Wang, *Chem. Commun.* **2015**, *51*, 3804–3807.
- [57] Y. Yang, Y. Wu, J.-H. Jia, X.-Y. Zheng, Q. Zhang, K.-C. Xiong, Z.-M. Zhang, Q.-M. Wang, *Cryst. Growth Des.* **2018**, *18*, 4555–4561.
- [58] S. Sanz, H. M. O'Connor, E. M. Pineda, K. S. Pedersen, G. S. Nichol, O. Mønsted, H. Weihe, S. Piligkos, E. J. L. McInnes, P. J. Lusby, E. K. Brechin, *Angew. Chem. Int. Ed.* **2015**, *54*, 6761–6764; *Angew. Chem.* **2015**, *127*, 6865–6868.
- [59] S. Sanz, H. M. O'Connor, P. Comar, A. Baldansuren, M. B. Pitak, S. J. Coles, H. Weihe, N. F. Chilton, E. J. L. McInnes, P. J. Lusby, S. Piligkos, E. K. Brechin, *Inorg. Chem.* **2018**, *57*, 3500–3506.
- [60] S. Sanz, H. M. O'Connor, V. Martí-Centelles, P. Comar, M. B. Pitak, S. J. Coles, G. Lorusso, E. Palacios, M. Evangelisti, A. Baldansuren, N. F. Chilton, H. Weihe, E. J. L. McInnes, P. J. Lusby, S. Piligkos, E. K. Brechin, *Chem. Sci.* **2017**, *8*, 5526–5535.
- [61] L. Li, Y. Zhang, M. Avdeev, L. F. Lindoy, D. G. Harman, R. Zheng, Z. Cheng, J. R. Aldrich-Wright, F. Li, *Dalton Trans.* **2016**, *45*, 9407–9411.
- [62] F.-S. Guo, B. M. Day, Y.-C. Chen, M.-L. Tong, A. Mansikkamäki, R. A. Layfield, *Angew. Chem. Int. Ed.* **2017**, *56*, 11445–11449; *Angew. Chem.* **2017**, *129*, 11603–11607.
- [63] S. Wang, J.-L. Zuo, H.-C. Zhou, H. J. Choi, Y. Ke, J. R. Long, X.-Z. You, *Angew. Chem. Int. Ed.* **2004**, *43*, 5940–5943; *Angew. Chem.* **2004**, *116*, 6066–6069.
- [64] P. Gütllich, A. Hauser, H. Spiering, *Angew. Chem. Int. Ed. Engl.* **1994**, *33*, 2024–2054; *Angew. Chem.* **1994**, *106*, 2109–2141.
- [65] R. W. Hogue, S. Singh, S. Brooker, *Chem. Soc. Rev.* **2018**, *47*, 7303–7338.
- [66] E. G. Percástegui, V. Jancik, *Coord. Chem. Rev.* **2020**, *407*, 213165.
- [67] T. Nakamura, H. Ube, R. Miyake, M. Shionoya, *J. Am. Chem. Soc.* **2013**, *135*, 18790–18793.
- [68] F. J. Rizzuto, D. M. Wood, T. K. Ronson, J. R. Nitschke, *J. Am. Chem. Soc.* **2017**, *139*, 11008–11011.
- [69] W. Brenner, T. K. Ronson, J. R. Nitschke, *J. Am. Chem. Soc.* **2017**, *139*, 75–78.
- [70] M. Yamashina, Y. Tanaka, R. Lavendomme, T. K. Ronson, M. Pittelkow, J. R. Nitschke, *Nature* **2019**, *574*, 511–515.
- [71] W. Meng, B. Breiner, K. Rissanen, J. D. Thoburn, J. K. Clegg, J. R. Nitschke, *Angew. Chem. Int. Ed.* **2011**, *50*, 3479–3483; *Angew. Chem.* **2011**, *123*, 3541–3545.
- [72] N. Struch, C. Bannwarth, T. K. Ronson, Y. Lorenz, B. Mienert, N. Wagner, M. Engeser, E. Bill, R. Puttreddy, K. Rissanen, J. Beck, S. Grimme, J. R. Nitschke, A. Lützen, *Angew. Chem. Int. Ed.* **2017**, *56*, 4930–4935; *Angew. Chem.* **2017**, *129*, 5012–5017.
- [73] M. B. Duriska, S. M. Neville, B. Moubaraki, J. D. Cashion, G. J. Halder, K. W. Chapman, C. Balde, J.-F. Létard, K. S. Murray, C. J. Kepert, S. R. Batten, *Angew. Chem. Int. Ed.* **2009**, *48*, 2549–2552; *Angew. Chem.* **2009**, *121*, 2587–2590.
- [74] H. Iranmanesh, K. S. A. Arachchige, M. Bhadbhade, W. A. Donald, J. Y. Liew, K. T.-C. Liu, E. T. Luis, E. G. Moore, J. R. Price, H. Yan, J. Yang, J. E. Beves, *Inorg. Chem.* **2016**, *55*, 12737–12751.
- [75] E. T. Luis, H. Iranmanesh, K. S. A. Arachchige, W. A. Donald, G. Quach, E. G. Moore, J. E. Beves, *Inorg. Chem.* **2018**, *57*, 8476–8486.
- [76] A. B. Wrage, A. J. Metherell, W. Cullen, M. D. Ward, *Dalton Trans.* **2015**, *44*, 17939–17949.
- [77] C. Colomban, C. Fuertes-Espinosa, S. Goeb, M. Sallé, M. Costas, L. Blancafort, X. Ribas, *Chem. Eur. J.* **2018**, *24*, 4371–4381.
- [78] Z. Wang, L.-P. Zhou, T.-H. Zhao, L.-X. Cai, X.-Q. Guo, P.-F. Duan, Q.-F. Sun, *Inorg. Chem.* **2018**, *57*, 7982–7992.
- [79] K. Li, L.-Y. Zhang, C. Yan, S.-C. Wei, M. Pan, L. Zhang, C.-Y. Su, *J. Am. Chem. Soc.* **2014**, *136*, 4456–4459.
- [80] A. J. Metherell, M. D. Ward, *Chem. Commun.* **2014**, *50*, 6330–6332.
- [81] A. K. Pal, B. Laramée-Milette, G. S. Hanan, *RSC Adv.* **2014**, *4*, 21262.
- [82] C. Schouwey, M. Pappmeyer, R. Scopelliti, K. Severin, *Dalton Trans.* **2015**, *44*, 2252–2258.
- [83] V. Chandrasekhar, R. Thirumoorthi, *Organometallics* **2007**, *26*, 5415–5422.
- [84] F. A. Cotton, L. M. Daniels, C. Lin, C. A. Murillo, *J. Am. Chem. Soc.* **1999**, *121*, 4538–4539.
- [85] J. K. Bera, R. Clérac, P. E. Fanwick, R. A. Walton, *J. Chem. Soc. Dalton Trans.* **2002**, 2168–2172.
- [86] W. Uhl, T. Spies, D. Haase, R. Winter, W. Kaim, *Organometallics* **2000**, *19*, 1128–1131.
- [87] A. Jana, S. Mandal, K. Singh, P. Das, N. Das, *Inorg. Chem.* **2019**, *58*, 2042–2053.
- [88] S. Ø. Scottwell, A. B. S. Elliott, K. J. Shaffer, A. Nafady, C. J. McAdam, K. C. Gordon, J. D. Crowley, *Chem. Commun.* **2015**, *51*, 8161–8164.
- [89] J. A. Findlay, C. J. McAdam, J. J. Sutton, D. Preston, K. C. Gordon, J. D. Crowley, *Inorg. Chem.* **2018**, *57*, 3602–3614.
- [90] J. D. Crowley, I. M. Steele, B. Bosnich, *Chem. Eur. J.* **2006**, *12*, 8935–8951.
- [91] S. Ø. Scottwell, J. E. Barnsley, C. J. McAdam, K. C. Gordon, J. D. Crowley, *Chem. Commun.* **2017**, *53*, 7628–7631.
- [92] I. Sinha, P. S. Mukherjee, *Inorg. Chem.* **2018**, *57*, 4205–4221.
- [93] W.-X. Gao, H.-N. Zhang, G.-X. Jin, *Coord. Chem. Rev.* **2019**, *386*, 69–84.
- [94] M. Otte, P. F. Kuijpers, O. Troeppner, I. Ivanović-Burmazović, J. N. H. Reek, B. de Bruin, *Chem. Eur. J.* **2013**, *19*, 10170–10178.
- [95] A. Gansäuer, M. Behlendorf, D. von Laufenberg, A. Fleckhaus, C. Kube, D. V. Sadasivam, R. A. Flowers, *Angew. Chem. Int. Ed.* **2012**, *51*, 4739–4742; *Angew. Chem.* **2012**, *124*, 4819–4823.
- [96] A. N. Oldacre, A. E. Friedman, T. R. Cook, *J. Am. Chem. Soc.* **2017**, *139*, 1424–1427.
- [97] S. S. Nurttila, R. Becker, J. Hessels, S. Woutersen, J. N. H. Reek, *Chem. Eur. J.* **2018**, *24*, 16395–16406.
- [98] H. Li, Y.-F. Han, Y.-J. Lin, Z.-W. Guo, G.-X. Jin, *J. Am. Chem. Soc.* **2014**, *136*, 2982–2985.
- [99] B. Roy, A. Devaraj, R. Saha, S. Jharimune, K.-W. Chi, P. S. Mukherjee, *Chem. Eur. J.* **2017**, *23*, 15704–15712.
- [100] J. Guo, Y.-W. Xu, K. Li, L.-M. Xiao, S. Chen, K. Wu, X.-D. Chen, Y.-Z. Fan, J.-M. Liu, C.-Y. Su, *Angew. Chem. Int. Ed.* **2017**, *56*, 3852–3856; *Angew. Chem.* **2017**, *129*, 3910–3914.
- [101] R. Saha, D. Samanta, A. J. Bhattacharyya, P. S. Mukherjee, *Chem. Eur. J.* **2017**, *23*, 8980–8986.
- [102] S. K. Samanta, J. W. Bats, M. Schmittel, *Chem. Commun.* **2014**, *50*, 2364–2366.
- [103] S. Saha, P. K. Biswas, M. Schmittel, *Inorg. Chem.* **2019**, *58*, 3466–3472.
- [104] N. Singh, S. Jang, J.-H. Jo, D. H. Kim, D. W. Park, I. Kim, H. Kim, S. C. Kang, K.-W. Chi, *Chem. Eur. J.* **2016**, *22*, 16157–16164.

Manuscript received: April 2, 2020

Revised manuscript received: April 14, 2020

Accepted manuscript online: April 15, 2020

Version of record online: September 11, 2020